

Small-scale stratification of the density field and its influence on the suspensions' concentration*

OCEANOLOGIA, 21, 1985
PL ISSN 0078-3234

Small-scale
stratification
Density field
Suspensions'
concentration

CZESŁAW DRUET, RYSZARD SIWECKI
Institute of Oceanology, Polish Academy of Sciences
Sopot

Manuscript received 14 May 1984, in final form 25 September 1984.

Abstract

The article presents the results of empirical investigations conducted during a cruise of the research vessel 'Profesor Siedlecki' in the Baltic in July 1980. They were aimed at establishing the relations between various characteristics of small-scale stratification of temperature, salinity, and velocity fields and the structure of vertical suspensions' distributions. The article presents detailed characteristics of the experiment hydrometeorological background and small-scale temperature field structure and the discovered correlations between the distributions of selected parameters characterizing the dynamics of small-scale stratification of the upper water layer (Cox number) and chlorophyll *a* concentration.

1. Object and goal of investigations

The results of several studies made in recent years, dealing with the turbulent diffusion of marine suspensions indicate that suspensions do not move in a manner similar to water elements**, but are subject to specific diffusion processes, which have a significant influence on the spatial-temporal changes of their concentration in the sea [1, 4]. These processes seem effectively influenced by the spatial-temporal mechanisms of 'tuning' of the layered structure of the density field and the velocity of water motion, manifest in the form of small-scale stratification (laminar-turbulent layers) registered on the profiles of the vertical distribution of these physical magnitudes as pulsatory non-homogeneities (Fig. 1). This small-scale stratification of hydrophysical fields is characteristic, as is well-known, of the whole sea, including the upper near-surface layer, which as a rule is conventionally treated as a homogeneous layer of density, temperature, and salinity.

* The investigations were carried out under the research programme MR. I. 15, coordinated by the Institute of Oceanology of the Polish Academy of Sciences.

** Element is understood in the article as the volume of water large enough to perform within it the operations of averaging of physical features and use the concept of suspensions' concentration and, at the same time, small enough to use the principles of differential equations for the description of motion.

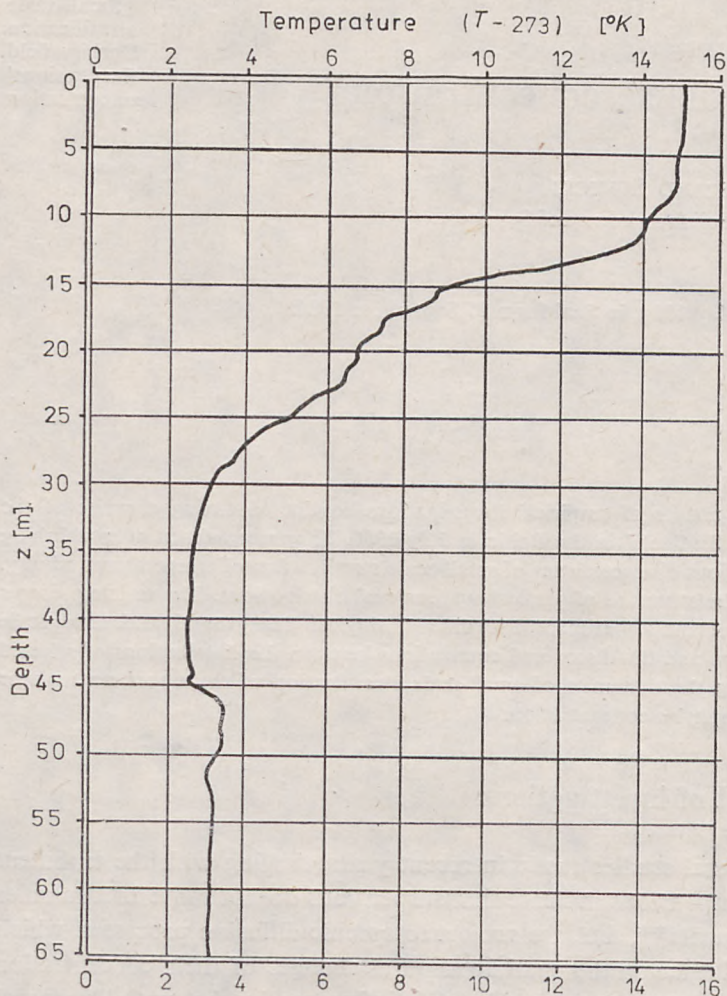


Fig. 1. Vertical distribution of momentary temperature values (example).

If the turbulent regime of water mass movement were homogeneous and the density at a given area were constant then, irrespective of the intensity of movement, suspensions' concentration would be more or less equally distributed in the water mass, if suspended substance had no autonomous ability to move and was characterized by neutral buoyancy. In the case of suspensions having an autonomous ability to perform vertical movements (*eg* plankton or heavy particles), the intensity of turbulence may only have an influence on the vertical velocity suspensions' movement. In no way can it have an influence on their concentration and spatial distribution.

Let us now imagine that basic hydrophysical fields of the sea are homogeneous only in the horizontal plane and the intensity of processes of turbulent exchange changes with depth. Empirical investigations have shown [3] that such vertical stra-

tification of the velocity and water density field is realized in the form of weakly turbulent homogeneous layers of varying thickness (from several centimetres to several metres), separated by thin (several centimetres thick) laminar layers, characterized by very strong gradients of hydrophysical features. Both the homogeneous turbulent layers and the laminar layers may, under proper conditions, change their structure, *ie* subdivide into smaller layers or change their thickness. That is why small-scale stratification most often manifests itself in the sea in the form of more complex vertical non-homogeneities [2, 3]. Under such circumstances, the intensity of the vertical flux of mass and energy transfer will change with depth and will depend on the density distribution and the dynamic properties of the stratified flow. These conditions will induce a non-homogeneous distribution of suspensions concentration, both mineral and planktonic.

The role of small-scale stratification of hydrophysical fields in the conditioning of biological processes in the sea seems significant. It is enough to realize that under the conditions of a homogeneous distribution of food suspensions concentrations, the amount of energy which zooplanktonic organisms would have to use up in search of food on their own would be much greater than the amount of energy obtained from the food found, and that only thanks to stratification these negative factors of life do not manifest themselves in a significant way.

Taking the above into consideration, long-term investigations were undertaken as part of problem MR. I. 15, aimed at finding the relations between the various characteristics of small-scale stratification of the temperature, salinity, velocity field and the structure of vertical distributions of suspensions' concentration in the sea. One of the tasks within the framework of the above mentioned programme was an experiment carried out in the Baltic in 1980 on the board of r/v 'Profesor Siedlecki', the research vessel of the Sea Fisheries Institute in Gdynia. The results obtained during this experiment constitute the subject matter of the present paper.

2. Methods and range of measurements

The peculiarities of small-scale stratification of hydrophysical fields are always induced on a certain general background, defined by mean hydrological properties of the sea, *ie* mean characteristics of density, temperature, salinity, gas content, current velocity fields. The knowledge of the spatial-temporal characteristics of these fields within the area of the experiment enables, on the one hand, the estimation of the intensity of advection and convection processes and their influence on the structure and dynamics of small-scale layers and, on the other hand, gives the basis for a rational simplification of differential equations of energy balance. The data referring to the characteristics of the density field were collected with Japanese made Ogawa Seiki reversible thermometers with attached bathometers and a continuous-recording bathythermograph. By means of this set of equipment, water samples were taken and its temperature was recorded every 20–30 minutes from the surface to the bottom with 10 m intervals. The salinity was

determined with a Plessey Environmental System (model 6230 N) salinometer. The measurements of directions and moduli of the resultant current velocities were made with autonomous BPW-2 digital current meters.

The investigations of the dynamic characteristics of small-scale stratification for the temperature field were conducted by means of thermistor equipment with a time constant $\tau \approx 0.16$ s and an effective resolution capability of continuous vertical recording $\Delta z = 3 \cdot \tau \cdot V_z = 0.4$ m. These measurements were made in the following way: a thermistor sensor was lowered vertically from the board of the anchored vessel with a mean sounding velocity $V_z = 0.9$ m/s from the ordinate -0.30 m to a depth covering the whole layer of the seasonal thermocline (50–60 m). These soundings were made every two minutes.

The main investigations were made from the anchored vessel at two long-term stations (Fig. 2): a ten-days station B_2 (July 6–August 15, 1980) and a seven-days station G_2 (July 21–July 27, 1980). Besides these long-term stations, some measurement series were also carried out at intermediate stations B_1, B_4, B_3, S_{10} and S_2 .

The empirical data registered during the expedition enabled, after processing, to obtain the vertical distributions of the following hydrophysical parameters:

- mean conventional density $\hat{\rho} = (\rho - 1) 10^3$ (where ρ is real density),
- mean chlorophyll *a* concentration,
- mean temperature (\bar{T}),
- mean salinity (\bar{S}),
- momentary temperature values (T),
- mean values of direction (A^0) and modulus $|\bar{u}|$ of water mass flow velocity at selected depths.

On the basis of above mentioned characteristics, the following parameters were calculated for each discrete layer Δz :

(i) mean vertical gradients of:

- temperature $\left(\frac{\Delta \bar{T}}{\Delta z} = \frac{\bar{T}_{z+\Delta z} - \bar{T}_z}{\Delta z} \right)$,
- conventional density $\left(\frac{\Delta \hat{\rho}}{\Delta z} = \frac{\hat{\rho}_{z+\Delta z} - \hat{\rho}_z}{\Delta z} \right)$,
- flow velocity $\left(\frac{\Delta \bar{u}}{\Delta z} = \frac{\bar{u}_{z+\Delta z} - \bar{u}_z}{\Delta z} \right)$;

(ii) Vaisala-Brunt frequency $\left(N^2 = \frac{g}{\rho_0} \cdot \frac{\Delta \rho}{\Delta z} \approx \frac{g}{10^3} \cdot \frac{\Delta \hat{\rho}}{\Delta z} \right)$;

(iii) dissipation velocity of subtle non-homogeneities:

$$\varepsilon_T = \chi_T \left(\frac{\Delta T^*}{\Delta z} \right)^2$$

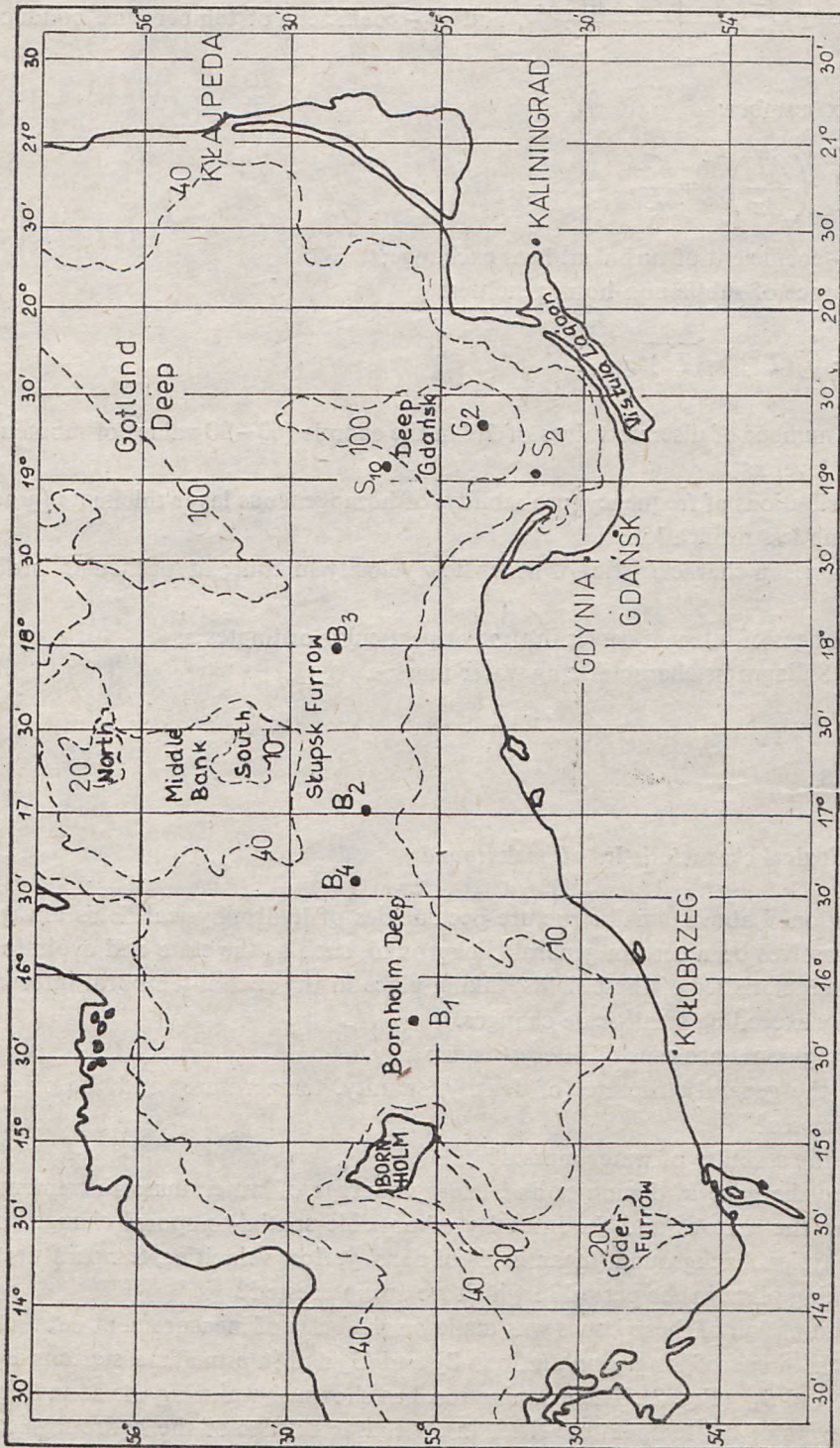


Fig. 2. Location of sampling stations in the Baltic during the 'Professor Siedlecki' expedition in 1980

where: $T^* = T - \bar{T}$, $\frac{\Delta T^*}{\Delta z} = \frac{T_{z+\Delta z}^* - T_z^*}{\Delta z}$, and χ_T —coefficient of temperature conductivity;

(iv) Cox number:

$$c_x = \left(\frac{\Delta T^*}{\Delta z} \right)^2 \cdot \left(\frac{\Delta \bar{T}}{\Delta z} \right)^{-2} = \frac{K_T}{\chi_T},$$

where: K_T —coefficient of turbulent heat exchange;

(v) variance of subtle non-homogeneities:

$$\sigma_T^2 = \frac{1}{n_z - 1} \cdot \sum_{i=1}^{n_z} (T^*)_i^2 = \overline{(T^*)^2},$$

where: n_z —number of discrete values of T^* in the sample (60–90 values of momentary T^*) at level z ;

(vi) distributions of frequency (probability) of homogeneous layer thickness (grad $T=0$) in subtle stratification;

(vii) changes in characteristics of water flow velocity in time; at particular ordinates z ;

(viii) changes of internal waves in time at particular ordinates z ;

(ix) $T-S$ diagrams characterizing water masses.

3. Results

3.1. Hydrological characteristics of background

As mentioned above, small-structure peculiarities of hydrophysical fields always realize themselves on a certain general background, such as the state and evolution of mean characteristics of these fields, taking place in the spatial-temporal interval considerably exceeding small-scale changes.

The following issues are thus of interest to us:

- what is the general structure (of density, salinity, temperature) and the origin of water masses?
- what is the stability of water masses?
- what are the general dynamics and energy sources of water mass movement?
- what are the reasons and the intensity of possible spatial-temporal changes of the hydrophysical background (mean fields of density, flow velocities, temperatures, salinity) taking place in the period in which we are interested?

The examination of these issues was made on the basis of measurement data recorded in the areas of long-term stations B_2 and G_2 and intermediate stations B_1 , B_4 , B_3 , S_2 , and S_{10} (Fig. 2). The examination has shown that during the soundings of subtle layers of the temperature field, mean characteristics of the hydrophysical

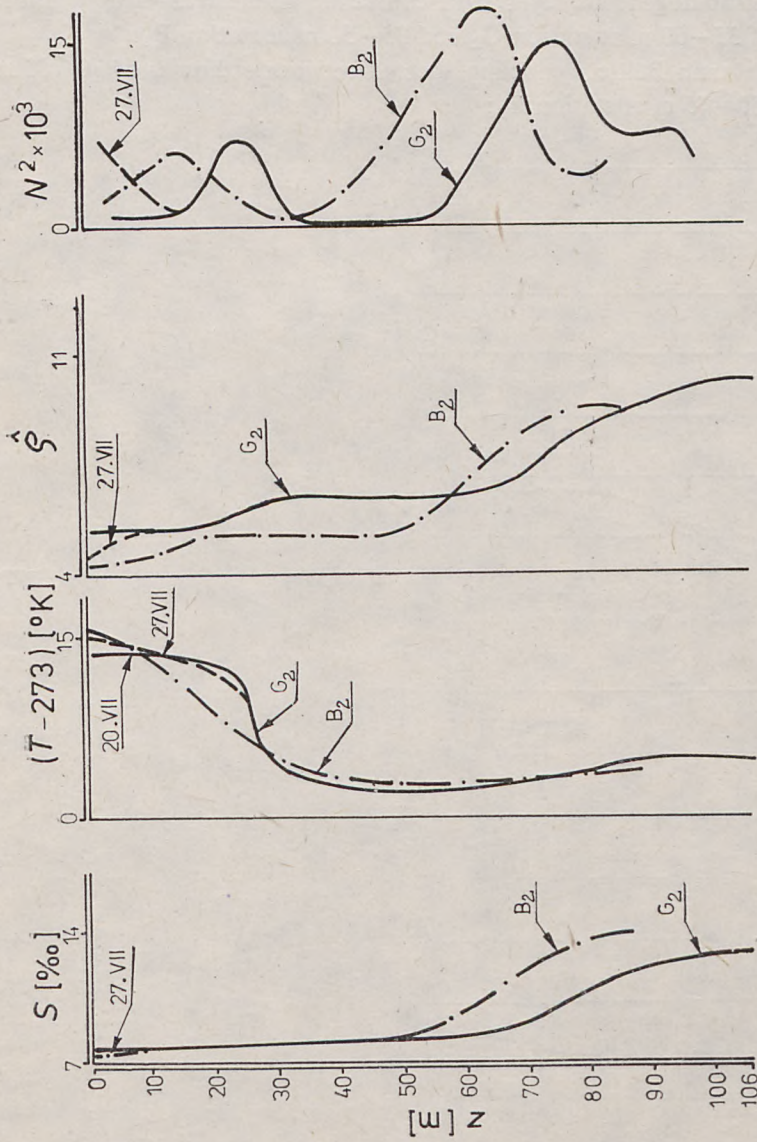


Fig. 3. Vertical distributions of mean characteristics of temperature field (\bar{T}), salinity field (\bar{S}), conventional density field ($\bar{\rho}$), and Vaisala-Brunt parameter (N^2) at station B₂ and station G₂ (typical characteristics for the whole experiments period)

background were more or less stationary and homogeneous in the horizontal plane in the study areas. In the vertical structure of density, salinity, and temperature fields, five main layers, differing in their hydrophysical structure, may be distinguished (Fig. 3):

(i) upper quasi-homogeneous layer, located in the Gdańsk Deep within the depth interval of 0.3–25 m, and in the Słupsk Furrow, within the depth interval of 0.3–15 m characterized by constant or almost constant values of parameters $\hat{\rho}$, \bar{T} , and \bar{S} ;

(ii) layer covering the seasonal pycnocline, located between ordinates of 25–30 m at station G_2 and 10 (15)–30 m at station B_2 ;

(iii) lower quasi-homogeneous layer with constant parameters, located in the ordinate interval of 35–60 m at station G_2 and 35–50 m at station B_2 ;

(iv) layer of the main Baltic pycnocline, located between ordinates of 70–85 m at station G_2 and 50–75 m at station B_2 ;

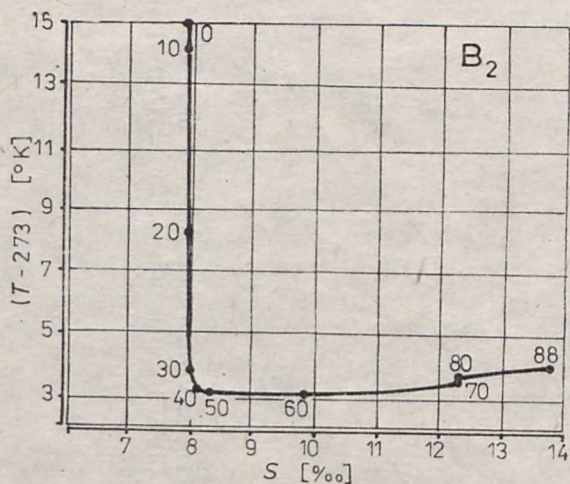
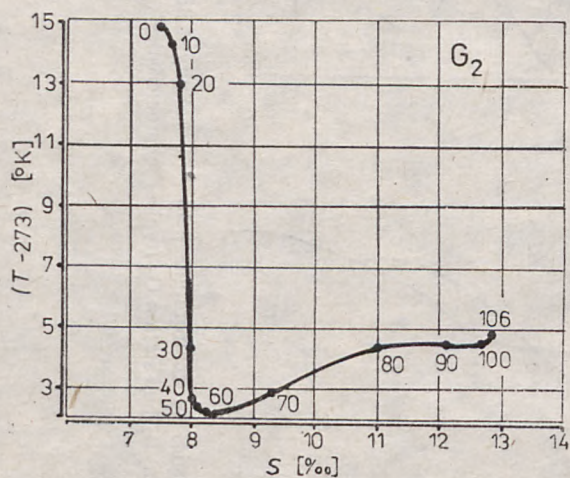


Fig. 4. Generalized $T-S$ diagrams for stations B_2 and G_2

(v) layer of near-bottom waters at depths below 85 m at station G_2 and below 75 m at station B_2 .

The analysis of $T-S$ diagrams (Fig. 4) confirmed the well-known fact of the presence at a depth of approximately 60 m in the Gdańsk Deep and approximately 50 m in the Slupsk Furrow of a thin layer, separating the main water masses of the Baltic: thermally changeable low-salinity Baltic waters (upper layer) and more saline North Sea waters, with almost constant temperature and changeable salinity.

Both the vertical distributions of parameters of mean field densities and the always positive values of Vaisala-Brunt parameter show that the area, in all its parts investigated during the expedition, was characterized by density stability from the free surface to the bottom. Although in the near-bottom layer a weak thermal inversion in temperature distribution was observed, it was compensated for by a stronger positive salinity gradient resulting in further density increase with depth.

It appears from wind characteristics recorded at station B_2 during the soundings starting on July 12, 1980 (Fig. 6) that in that period we had very weak winds: oscillations of their velocities could not have caused any major changes in the structure of water masses. Therefore, the distributions presented in Figure 3 may be thought as characteristic of the whole period during which vertical stratificational soundings were made at station B_2 . The stability of hydrophysical conditions at station G_2 was slightly different during the period of investigations. Weak winds were observed only during the first two days of investigations (July 20 and 21, 1980, Fig. 6). In the night of July 21/22, wind velocity increased about twice to 8–10 m/s and remained at this level until the end of investigations (July 26, 1980). This change in wind conditions might have caused certain small changes in the density distribution of the near-surface water layer in the last two days of investigations. However, the main reason for these changes seems not to be an increase in the intensity of turbulent momentum exchange processes in the upper water layer but a change in the thermal conditions in the near-water layer of atmosphere and changes in the salinity of the near-surface water layer, caused by precipitation. The decrease in water density, caused by these factors (Fig. 3) resulted in an increase in the stability of water masses as indicated by the increase of positive values of Vaisala-Brunt parameter.

Let us now make an evaluation of the water mass dynamics. The main problem of interest in this respect is the spatial-temporal changeability and energy sources of advection processes. Figure 5 presents diagrams of changes in time of moduli and directions of water flow velocities at station G_2 on July 21, 1980, recorded at ordinates -15 m, -40 m, and -60 m. These diagrams show the oscillation character of changes of mean flow velocities characterized by two time scales, differing from each other by one order of magnitude. One of them has hour periods ($T_1 \approx 12-14$ hours), the other minute periods ($T_2 \approx 20-40$ min). These two different oscillations have different sources. Since the moduli and directions of azimuth (A^0) of water flow velocity on ordinates -40 and -60 m are almost identical (Fig. 5), further analysis may be conducted on the basis of flow characteristics at the levels of -15 and -40 m. The reason for long-term oscillations seems to lie in quasi-periodic

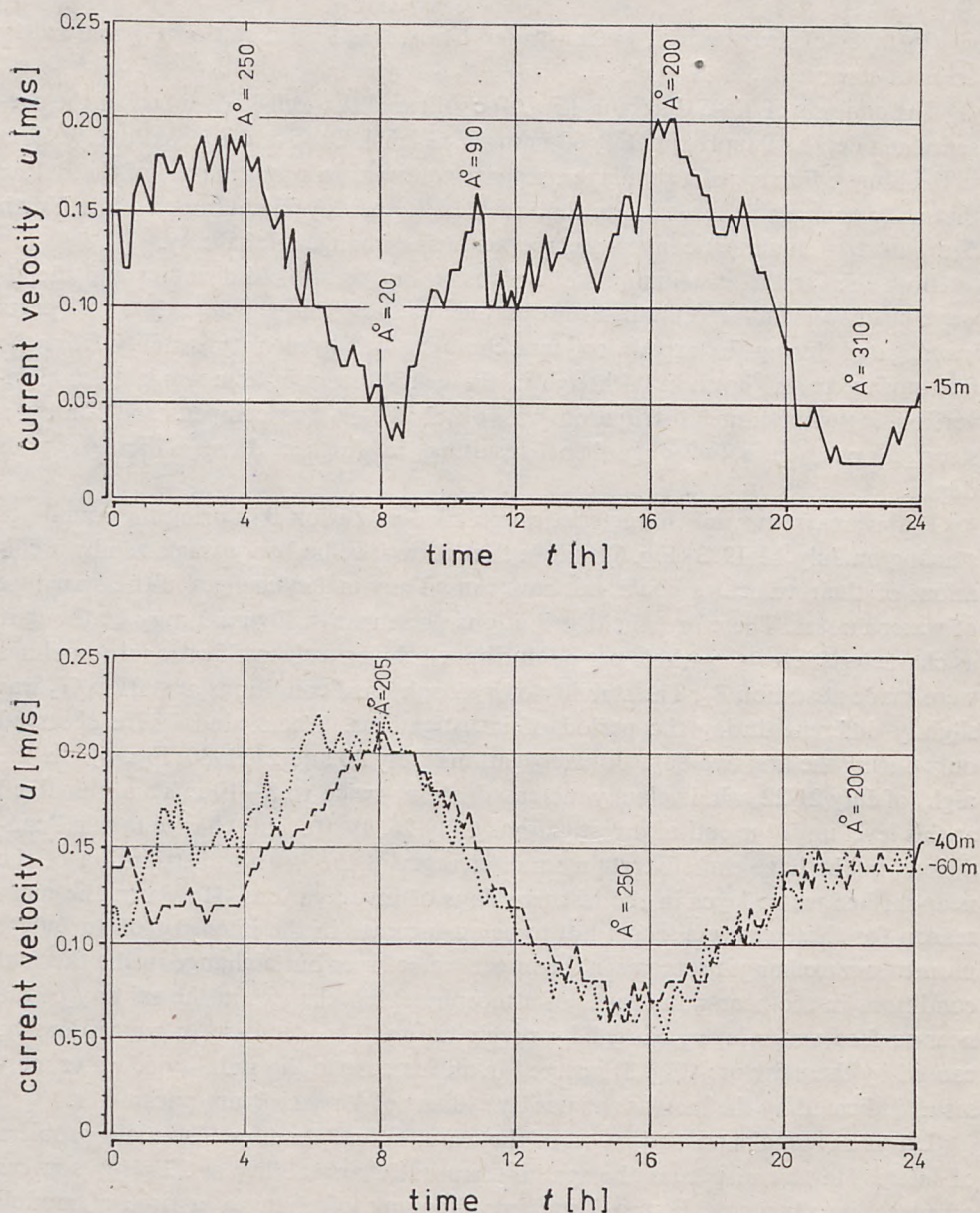


Fig. 5. Changes in time of mean velocities of water mass flow (\bar{u}) at depths of $z_1 = -15$ m, $z_2 = -40$ m, and $z_3 = -60$ m at station G_2

oscillations of wind velocity. Diagrams presented in Figure 6 confirm this quite clearly. In this figure, the same numerals designate the extrema corresponding to the concrete extremum of wind velocity. Ordinate of -15 m is located above the seasonal pycnocline and ordinate of -40 m—below it. The change in wind velocity will be noticed on ordinate of -15 m after 6 ± 2 hours and much later on ordinate of -40 m. Thus, between the moments of occurrence of particular extrema on ordi-

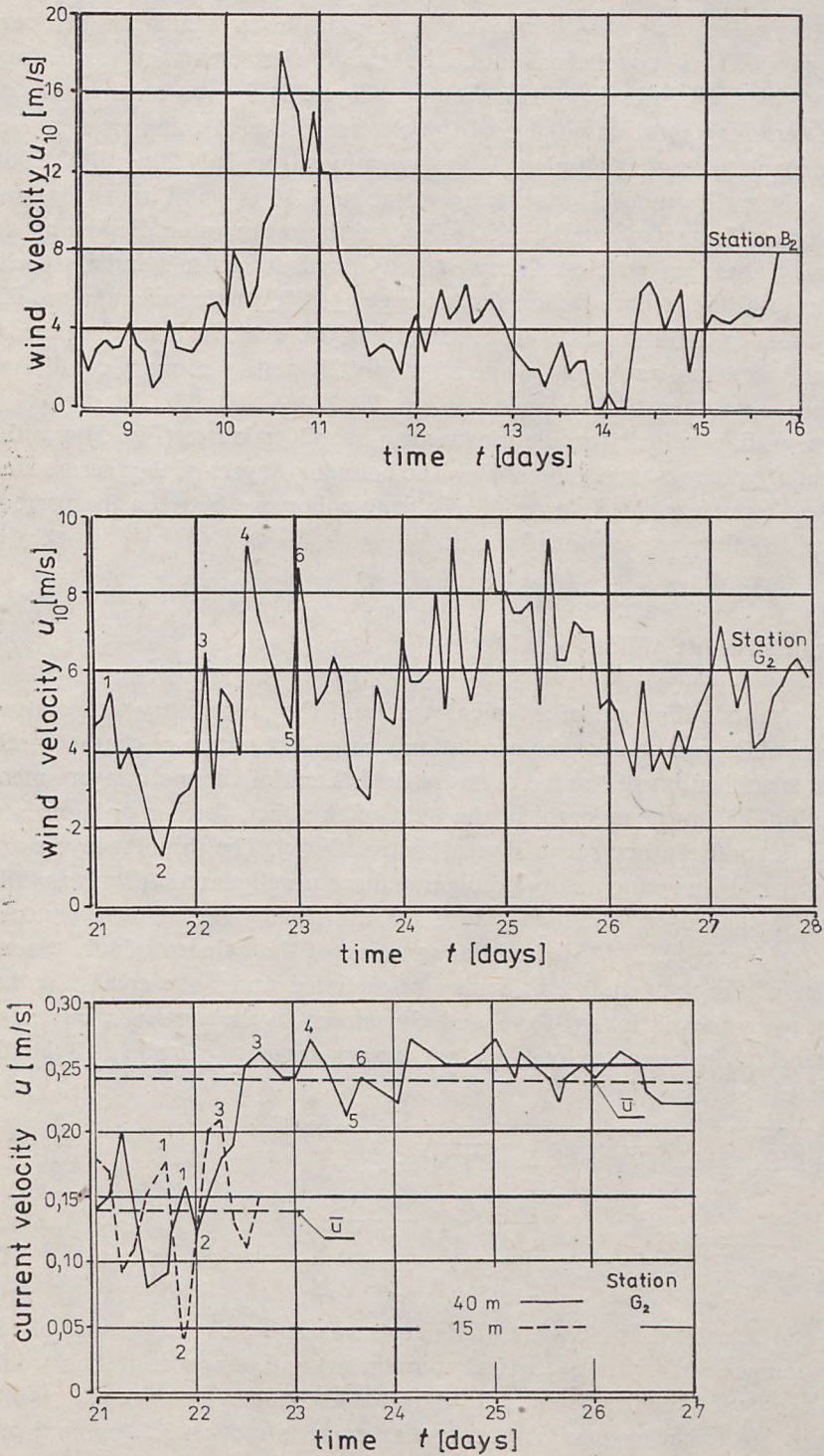


Fig. 6. Changes in time of wind velocity moduli (u_{10}) and current moduli (\bar{u}) at stations G₂ and B₂

nate of -15 m and ordinate of -40 m, phase shifts must occur, which can be clearly seen in Figure 6. These conclusions should be treated with reservations since they were based on relatively little data from the upper layer. Still, even on the basis of these data, a certain general knowledge of the characteristics of water mass movement may be acquired. In the first phase of investigations from July 20 until 22, 1980 (12.00), mean diurnal value of flow velocity was about 0.14 m/s and its oscillations over several hours fluctuated around $\pm 30-70\%$ of the mean value. Beginning on July 22 (evening hours) mean diurnal flow velocity reached 0.24 m/s and its oscillations over several hours equalled on the average $\pm 20\%$ of the mean value. We may thus say that in the first phase of investigations the weak turbulent regime of the background was non-stationary, while after July 23 quasi-stationary conditions were observed.

The source of flow velocity oscillations lasting over 10 minutes (Fig. 5) was the orbital motion of gravity waves, generated in the boundary layers of the thermocline (internal waves), which is clearly a result of strong coherence between the periods of these waves and flow velocity oscillations.

3.2. Small-scale structure of density field

Figure 1 presents a diagram of a typical profile of the momentary temperature distribution, in which one can see the oscillation or step-like structure characteristic of small-scale stratification of the temperature field. Each of the main layers mentioned in section 3.1. must undergo, in the light of this fact, further division into thinner layers (several centimetres to several metres thick). The thinnest layers are characterized by a strong temperature gradient and are usually laminar layers, while homogeneous, thicker layers in which $\text{grad } T \approx 0$, are usually turbulent layers to a lesser or greater degree [2, 3]. A differential equation of the balance of subtle non-homogeneities of the temperature field may be assumed under the conditions investigated by us in the stationary form and considered in the vertical plane x, z (axis x is parallel to the current velocity vector), always arranged parallelly to the direction of advective flow [6]:

$$\begin{aligned} \bar{u} \cdot \frac{\partial(T^*)^2}{\partial x} + \bar{w} \frac{\partial(T^*)^2}{\partial z} + \frac{\partial}{\partial x} \overline{u^*(T^*)^2} + \frac{\partial}{\partial z} \overline{w^*(T^*)^2} + \\ + 2\bar{u}^* T^* \cdot \frac{\partial \bar{T}}{\partial x} + 2\bar{w}^* T^* \cdot \frac{\partial \bar{T}}{\partial z} = -2\chi_T \left[\left(\frac{\partial T^*}{\partial x} \right)^2 + \left(\frac{\partial T^*}{\partial z} \right)^2 \right] \end{aligned} \quad (1)$$

where: \bar{u} , \bar{w} , and \bar{T} , as well as u^* , w^* , and T^* are mean and pulsatory values of the velocity field components (w is the vertical component) and temperature field components, while χ_T is the coefficient of molecular heat exchange.

The analysis of the background characteristics made in section 3.1. pointed out to the horizontal homogeneity of the features characterizing the layered structure of hydrophysical fields. Under these conditions, horizontal temperature gradients

will approach zero and equation (1) will have the form:

$$\bar{w} \cdot \frac{\partial (\overline{T^*})^2}{\partial z} + \frac{\partial}{\partial z} \overline{w^* (T^*)^2} + 2 \cdot \overline{w^* T^*} \cdot \frac{\partial \bar{T}}{\partial z} = -2\chi_T \cdot \left(\frac{\partial T^*}{\partial z} \right)^2 \quad (2)$$

The first term of this equation, which expresses the vertical advection of mean-square temperature deviation in the mean flow always assumes values incomparably smaller than the values of the remaining terms of equation (2) due to the small values of the mean velocity of vertical flow \bar{w} (in the order of 10^{-6} m/s). Because of this small value, it may be disregarded in further considerations. We may do the same with the second term of the equation representing the divergence of turbulent flux of non-homogeneities. As a result, we shall obtain a formula expressing an equilibrium or interpenetration of temperature non-homogeneities generation processes, caused by turbulent erosion of the mean temperature gradient and dissipation of these non-homogeneities (left side of the equation):

$$2\overline{w^* T^*} \cdot \frac{\partial \bar{T}}{\partial z} = -2\chi_T \cdot \left(\frac{\partial T^*}{\partial z} \right)^2 \quad (3)$$

Thus, Cox number characterizing the turbulent heat exchange and conditioning the mechanism of 'tuning' of this stratification will constitute the main criterion of their dynamics evaluation [6].

Figures 7–10 present examples of the vertical distributions of statistical characteristics showing the state and dynamics of subtle stratification of the temperature field at stations B_1 , B_2 , B_3 , B_4 , S_2 , S_{10} and G_2 . They refer to mean temperature values, intensity of turbulent heat exchange, and the dissipation of subtle non-homogeneities. Since it appears from the background characteristics (Fig. 3) that up to a depth of 60 m, the vertical distributions of mean salinity values may be treated as homogeneous, then subtle stratification of the temperature field must cause a similar stratification of the density field. It can be seen from diagrams in Figure 7–10 that in the main pycnocline layer ($\text{grad } \bar{T} = \text{max}$) we encounter quasi-laminar processes, characterized by an overwhelming influence of the molecular momentum exchange. In the layers located above and below the ocline, the values of Cox number are usually greater than one ($\log Cx > 0$). The investigations of the vertical distributions of the temperature pulsations variance and the strong maxima in the distribution of dissipation velocity shown in Figure 7–10 irrefutably point out to the fact that in the thermocline layer we have strong non-homogeneities, caused by the kinematic effect of internal waves. This is also indicated by the extreme significant values of Vaisala-Brunt parameter (Fig. 3). Under these conditions, a number of characteristics investigated by us should be functionally related to the kinematics of internal waves. In the first place, this should refer to Cox number and vertical temperature gradient. Taking into account the fact that the root of Vaisala-Brunt parameter characterizes the boundary frequencies of internal waves, we may look for the dependences $Cx = f_1(N)$ and $\frac{\partial \bar{T}}{\partial z} = f_2(N)$, whose

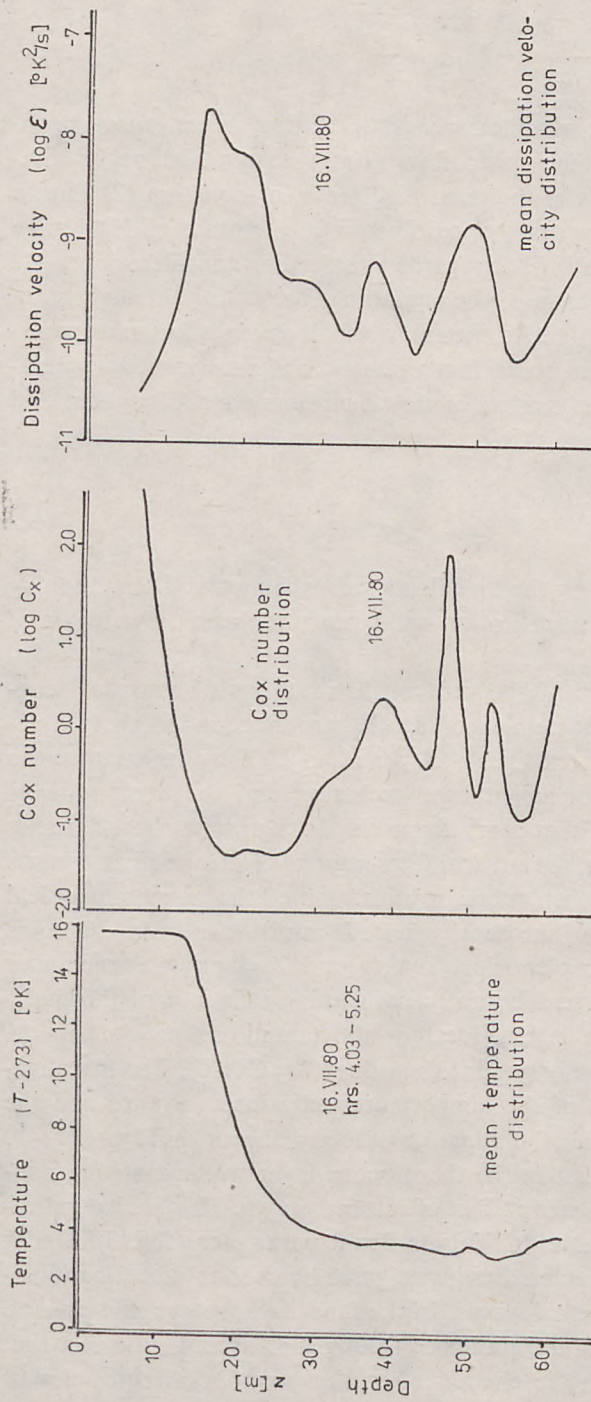


Fig. 7. Vertical distributions of mean temperature (\bar{T}), Cox number (C_x), and mean dissipation velocity of temperature non-homogeneities ($\bar{\epsilon}_T$) at station B_1 (averaged time of sampling was 1 hour 22 min)

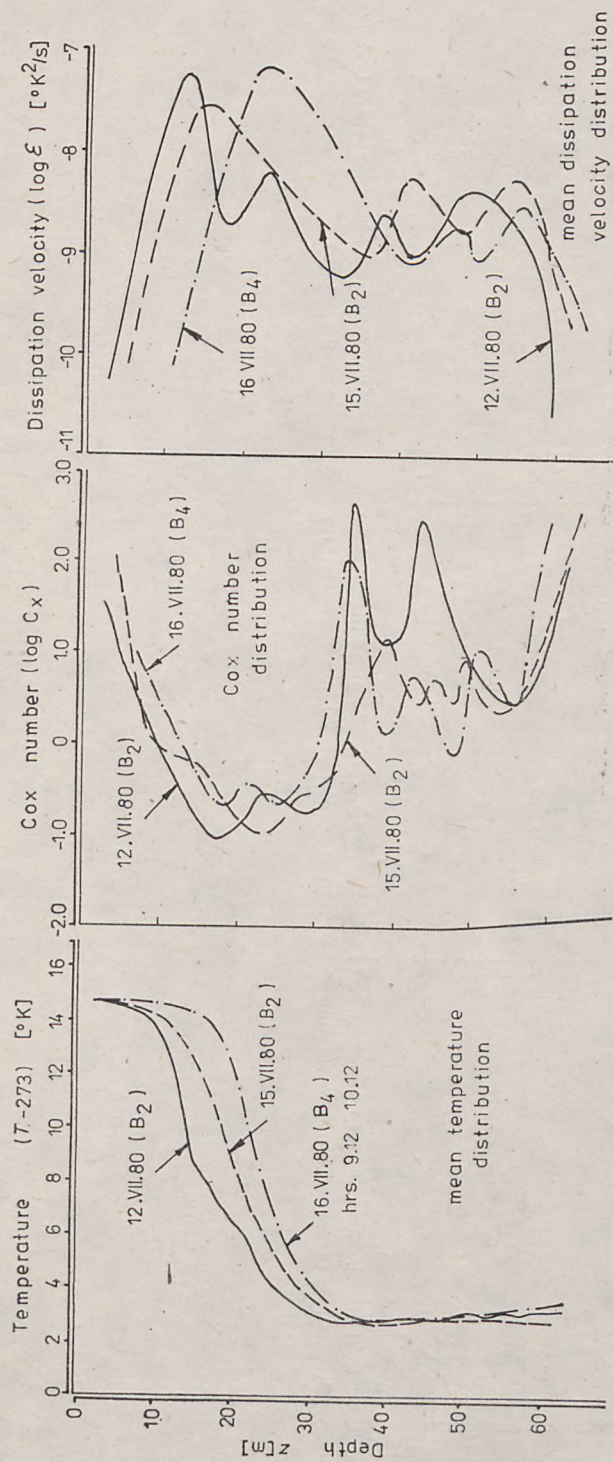


Fig. 8. Vertical distributions of mean temperature (\bar{t}), Cox number (C_x), and mean dissipation velocity of temperature non-homogeneities ($\bar{\epsilon}_T$) at stations B_2 and B_4 (averaged time of sampling was 2 hours 17 min at station B_2 and 2 hours at station B_4)

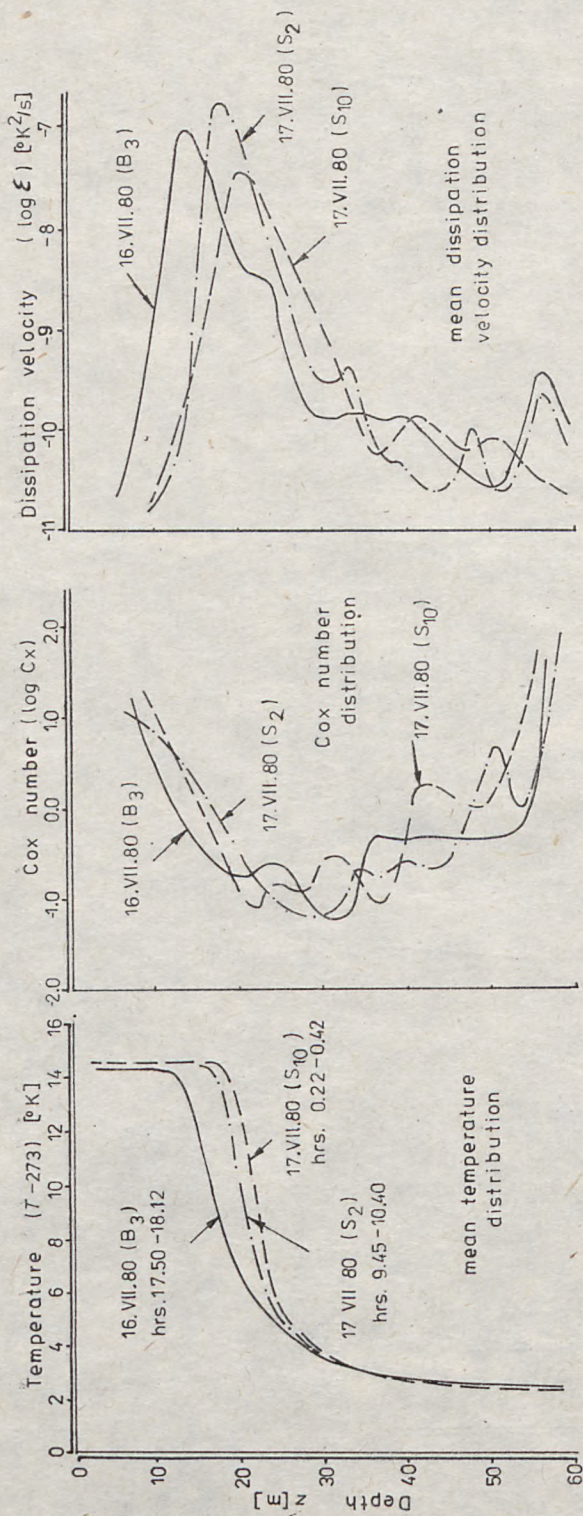


Fig. 9. Vertical distributions of mean temperature (\bar{T}), Cox number (Cx), and mean dissipation velocity of temperature non-homogeneities ($\bar{\epsilon}_T$) at stations S₂, S₁₀, and B₃ (averaged time of sampling was 44 min at station S₂, 20 min at station S₁₀, and 22 min at station B₃)

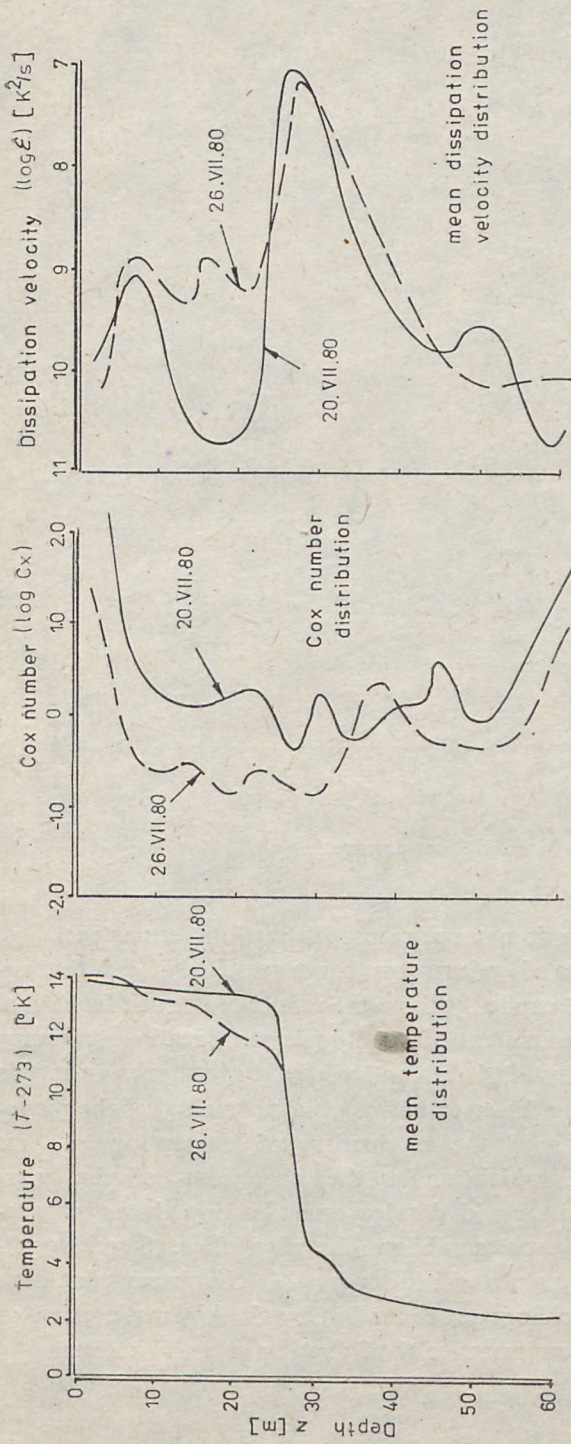


Fig. 10. Vertical distributions of mean temperature (\bar{T}), Cox number (C_x), and mean dissipation velocity of temperature non-homogeneities ($\bar{\epsilon}_T$) at station G_2 (averaged time of sampling was 2 hours 10 min)

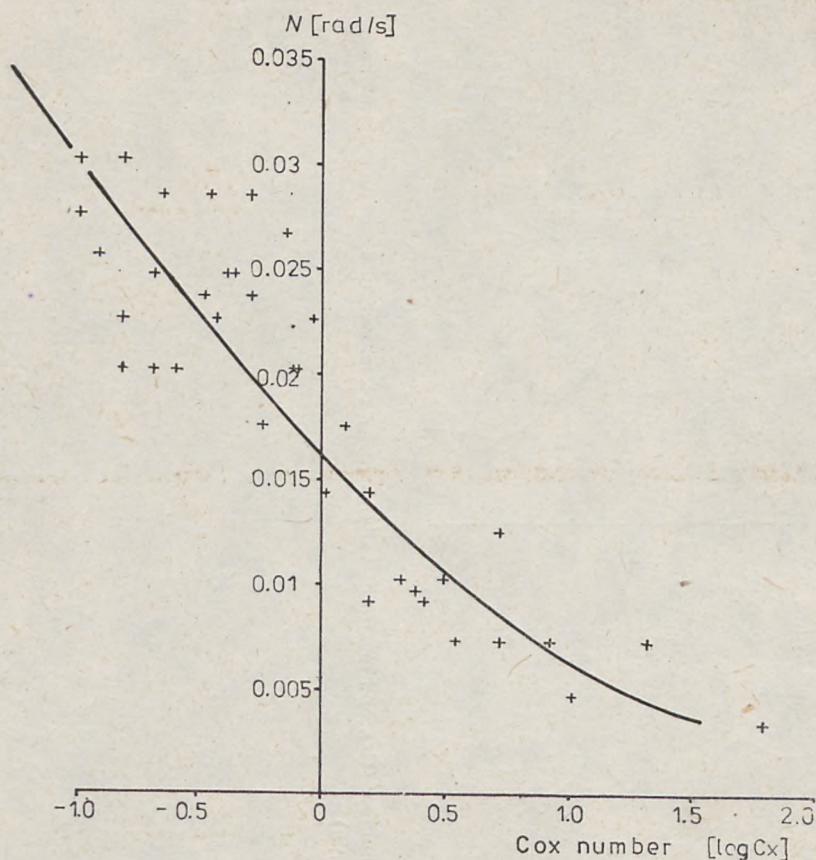


Fig. 11. Dependence of Cox number on Vaisala-Brunt parameter

existence would in fact attest to the dominance of processes of molecular exchange in the pycnocline layer. The examples of typical regression curves for these dependences, presented in Figures 11 and 12, explicitly show the existence of such functional relations between the dynamic parameters of small-scale stratification. We may thus say that besides gravity, density lift forces and viscosity of water were in this period the main factors conditioning the mechanisms of layer 'tuning' of the pycnocline. These factors effectively shaped the mechanism of absorption of this part of the advective energy, which under the conditions of the overwhelming influence of inertial forces could develop turbulence in the homogeneous layers more intensively and even annihilate the pycnocline. Strong oscillations of momentary temperature values which appeared in the thermocline area were not induced by turbulent exchange processes but by the kinematic effect of internal waves, whose mean height approached the following value (Fig. 13):

$$\bar{H}_w = \sigma \left(\frac{\Delta \bar{T}}{\Delta z} \right)^{-1} \approx 0,7m.$$

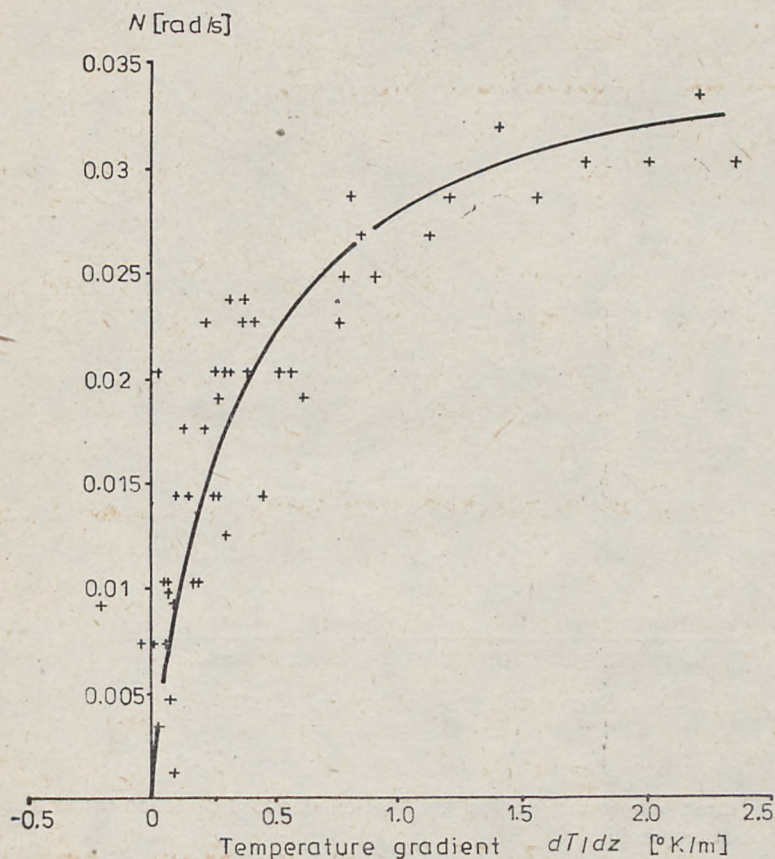


Fig. 12. Dependence of mean temperature vertical gradient on Vaisala-Brunt parameter

This estimation is obviously an approximate one, since the above dependence is based on Prandtl's hypothesis of mixing lengths in turbulent motion, according to which $T^* \sim l \frac{d\bar{T}}{dz}$. Thus, the characteristic scale of the mixing length equals

$l \sim T^* \frac{d\bar{T}^{-1}}{dz}$. In the case of the kinematic effect of internal waves, the orbital velocities

of water movement are the dominant mixing factors. Thus, the mean scale of the mixing length may be expressed by the mean height of these waves \bar{H}_w . For comparison, it may be mentioned that this relation within the oceanic thermocline assumes values ranging from 1 to 10 m. In the 24-hours thermocline, according to the results of our investigations in the Black Sea, this relation fluctuates between $\bar{H}_w \approx 0.3-0.5$ m.

Let us now consider the dynamics of changes in small-scale stratification of the density field above and below the pycnocline. The distributions of Cox number and dissipation velocities of subtle non-homogeneities, presented in Fig 7-10, show that the dynamics in these areas is very similar. Both the small values of Cox number

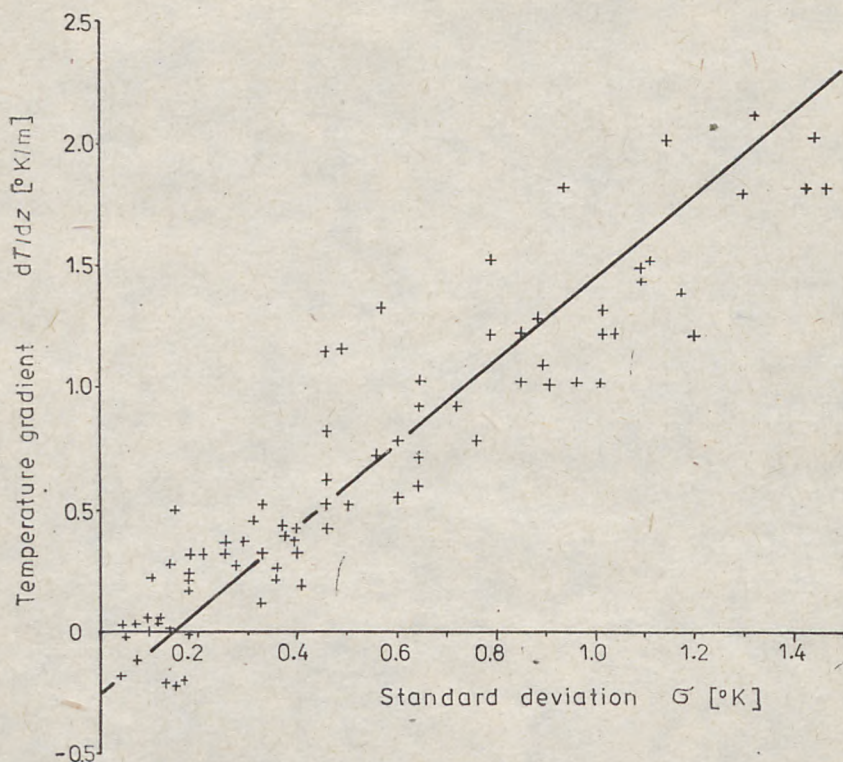


Fig. 13. Dependence of mean temperature vertical gradient on standard deviation (σ) of temperature field subtle non-homogeneities

and relatively small differences in dissipation velocities of small-scale non-homogeneities indicate that in the whole area of the stratified density field adjacent to the thermocline, homogeneous layers (extreme values of $C_x > 1$) are characterized by weak turbulence. Only in the near-surface area we have a homogeneous layer about 6 m thick, which is characterized by more intensive, turbulent exchange. In the period of investigations, the layered structure of the temperature field underwent evolutionary changes, which caused permanent restructuring of subtle layers, as signified by changes in the distributions of frequency of homogeneous layers thickness ($\text{grad } \bar{T} \approx 0$) occurrence. For example, in the first stage of soundings near station G_2 , layers with a thickness of over 6 m had a considerable share in the layered structure of the temperature field; later they were subdivided into thinner layers. This active restructuring was especially visible in the upper layer where two weak thermoclines appeared after two days (Fig. 10). The subdivision of the laminar layers was caused under these conditions by Kelvin-Helmholz instability, resulting from the overlapping of the orbital velocity of internal waves with the velocity of drift laminar water flow. The microturbulence generated as a result of this hydrodynamic instability split the main laminar layer into two parts, separated by a newly-formed homogeneous layer of weak turbulence. Homogeneous layers of considerable thickness were split into thinner layers either as a result of the influence of intrusion processes

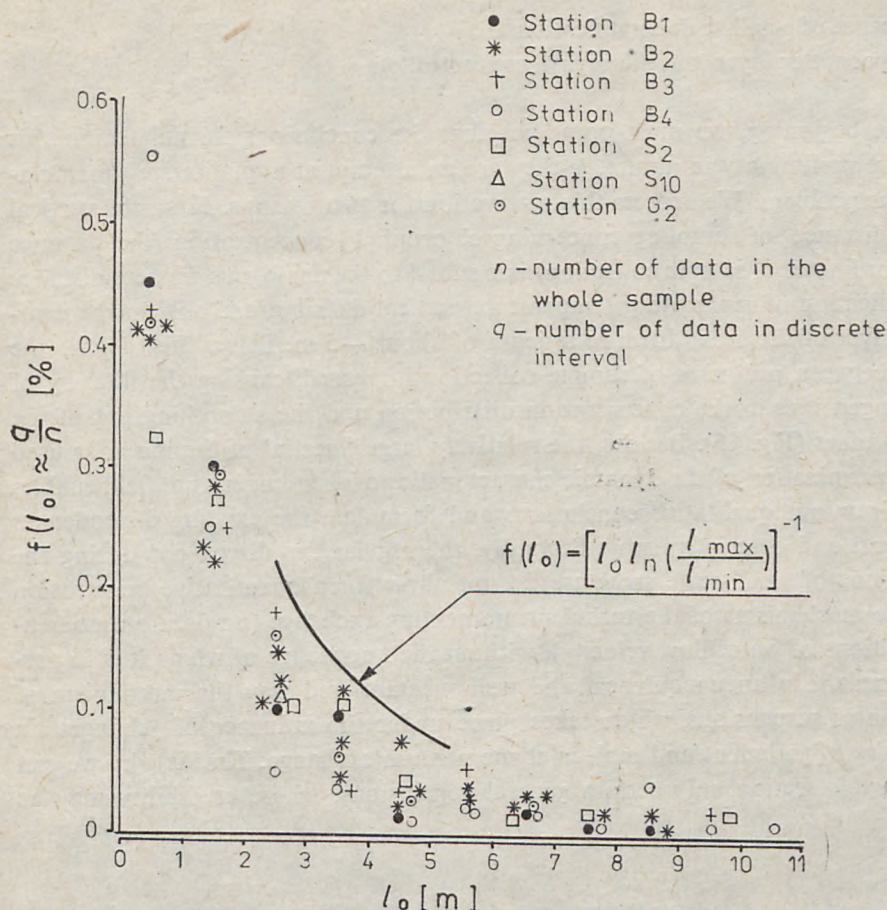


Fig. 14. Distributions of empirical density functions of probability of homogeneous layers thickness occurrence

or the disappearance of turbulence in the layer and the appearance of subtle structures with internal waves.

The theoretical estimator of the density of probability function for turbulent homogeneous layers $f(l_0)$, where l_0 is the thickness of the homogeneous layer, in the small-scale stratification of the Baltic waters, investigated by us, may be formulated similarly as in the oceanic thermocline, in which this distribution is subject to the logarithmic-normal law (Fig. 14):

$$f(l_0) = \frac{1}{\sigma \sqrt{2\pi}} \exp \left\{ -\frac{[\ln(l_0) - \overline{\ln(l_0)}]^2}{2\sigma^2} \right\},$$

which can be particularly described by a hyperbolic-type distribution:

$$f(l_0) = [l_0 \cdot \ln(l_{\max} \cdot l_{\min}^{-1})]^{-1}$$

where: l_{\max} and l_{\min} are the greatest and the smallest thickness of the homogeneous layer in the sample.

3.3. Influence of small-scale stratification of the upper water layer on chlorophyll concentration

At the beginning, we must point out that the conclusions formulated in this section are preliminary in nature, *ie* they are an attempt at a qualitative formulation of the problem. We express this reservation for two reasons. First, the vertical discrete distance of sampling concerning chlorophyll concentration (the distance between ordinates of sample collection) was suited to the analogous discrete distance of quantification of momentary temperature vertical distributions only in the near-surface layer of the area, down to a depth of about ~ 5 m. Below this depth, the distance between ordinates of sample collection increased, causing the filtering of non-homogeneities in the concentration distribution and the smoothing out of the vertical profiles (Fig. 15). Besides, the relatively large 'inertia' of the methods used for the determination of the dynamic characteristics of the temperature field enables only to draw out qualitative conclusions and formulate the existing dependences in a general and descriptive way. Secondly, the regularities discovered during the investigations of small-scale structure do not allow for a quantitative penetration microscale mechanisms of the turbulent momentum exchange (no data on momentary pulsations of water flow velocity), without the knowledge of which it is impossible to explain in an unequivocal and well substantiated way the mechanism of segregation of suspensions, which takes place under the influence of changes in the intensity of turbulent and molecular momentum exchange. That is why we can present in this section only certain general conclusions, whose credibility may be

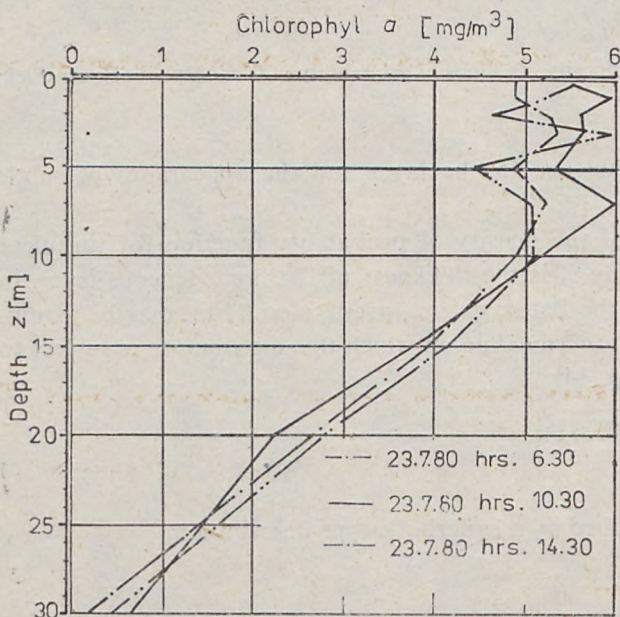


Fig. 15. Vertical distributions of chlorophyll *a* concentration values (example)

supported by further studies. These reservations do not, of course, depreciate the importance of the problem discussed in section 1; the investigations made and their conclusions may be of considerable importance for further studies of environmental factors of biological processes in the sea.

Typical exemplary vertical distributions of chlorophyll *a* concentration, presented in Figure 15, show a distinct decrease in concentration with depth and the oscillation character of changes in the upper 10 m layer, where samples were taken every metre. We can see also that in the time intervals separating particular distributions, there were no significant qualitative changes in the set-up of the extrema of these oscillations, which confirms their conservative nature with respect to time. Among the set of distributions of this kind, obtained during the investigations, only those distributions which were characterized by the same or similar period of stratified sounding were selected for comparisons.

A comparison of the distributions of particular parameters characterizing the

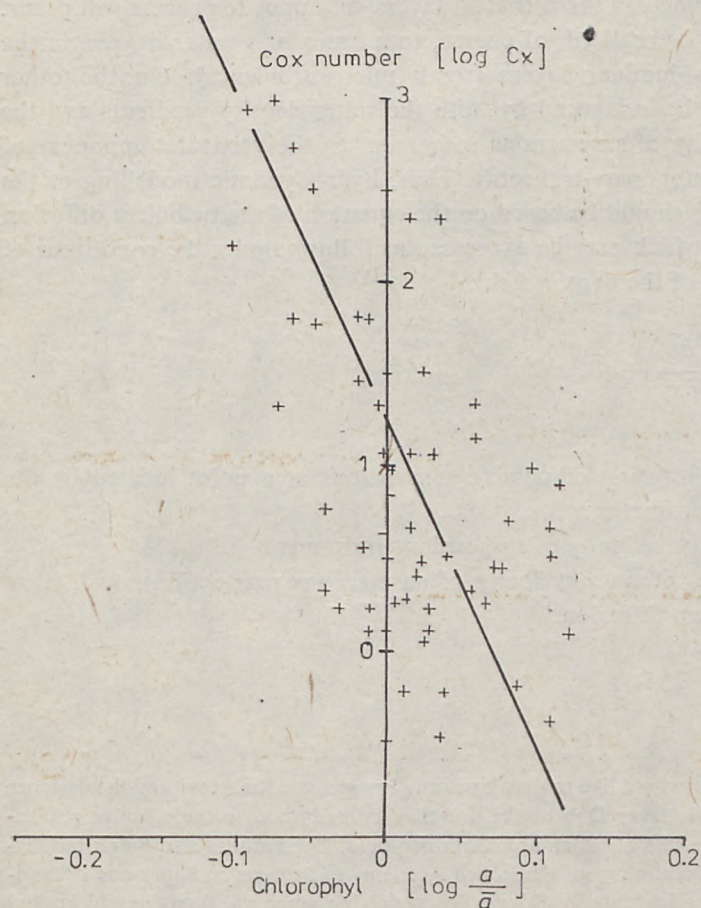


Fig. 16. Dependence of relative chlorophyll *a* concentration on Cox number in the near-surface layer

dynamics of small-scale layers with the chlorophyll *a* concentration distributions in the upper 10 m layer show that not all of these parameters exhibit satisfactorily distinct properties which would be coherent with concentration distributions. The most unequivocal in this respect is Cox number. The empirical regression function presented in Figure 16 suggests that there must be functional dependences between Cox number and the relative non-dimensional chlorophyll concentration a/\bar{a} , where \bar{a} is the averaged value for the segment $\Delta z = 10$ m.

In the light of hydrodynamic laws, this regularity may exist only in one case, *ie*, when a considerable portion of discrete suspensions will not have neutral buoyancy and will be under the overwhelming influence of either gravity or density lift forces. In the first case, suspensions will tend to move downwards, in the latter—upwards. In either case, the turbulent layers (characterized by intensive momentum exchange) will strengthen these tendencies while the laminar layers will weaken them. As a result, in the laminar layers ($Cx \ll 1$), a drop of mean velocity of the suspensions movement carried by advection of mean water flow and an increase in concentration will take place; in the turbulent layers, an opposite process will occur. This regularity will also be realized, of course, to a lesser or greater degree, in the quasi-turbulent or quasi-laminar layers (weak microturbulence). On the other hand, this process must be influenced by both the water density gradients and the ratio of the mean velocity of suspensions movement to the vertical component of advection velocity of water mass transport. Thus, hydrodynamic modelling of the above-mentioned process should be based on the equation of the turbulent diffusion of a discrete substance, which may be expressed as follows under the conditions of small-scale stratification of the density field:

$$\frac{\partial \bar{g}}{\partial t} + \frac{\partial}{\partial x_i} (\bar{u}_i \bar{g}) = \frac{\partial}{\partial x_i} \left(K_g \frac{\partial \bar{g}}{\partial x_i} \right) + q \bar{g},$$

where:

\bar{g} —mean value of concentration of passive suspensions at a point located by the vector of generalized coordinates x_i ,

\bar{u}_i —vector of mean relative velocity of suspensions movement,

q —coefficient of source intensity (velocity of suspensions production),

K_a —coefficient of turbulent diffusion.

Acknowledgments

The authors of this paper would like to thank warmly Mr Henryk Kućmierz and the designer of sensitive thermographs, Mr Jerzy Dąbrowski, for their contribution to the effective realization of the experiment, the results of which are contained here. The authors also thank biophysicists from the Institute of Oceanology of the Polish Academy of Sciences in Sopot and oceanographers of the Sea Fisheries Institute in Gdynia for supplying empirical data on chlorophyll *a* concentration and hydrological characteristics of the background.

References

1. Dera J., 1983, *Fizyka morza*, PWN Warszawa.
2. Druet C., Siwecki R., 1983, *Subtelna struktura hydrofizycznych pól w morzu – Eksperyment 'Kamczija-77'*, Stud. i Mater. Oceanol. KBM PAN, 40.
3. Fedorov K. N., 1976, *Tonkaia termokhalinnaia struktura vod okeana*, Gidrometeoizd. Leningrad.
4. Jerlov N. G., 1959, *Maxima in the vertical distribution of particles in the sea*, Deep-Sea Res., 5.
5. *Okeanologia. Ch. I. Gidrofizika*, 1979, Nauka, Moskva.
6. Riley G. A., Stommel H., Bumpus D. F., 1949, *Quantitative ecology of the plankton of the Western North Atlantic*, Bull. Bingham. Oceanogr. Coll., 12.